Wigner distribution of a general angular-momentum state: Applications to a collection of two-level atoms

Jonathan P. Dowling
Weapons Sciences Directorate, AMSMI-RD-WS-ST, Research, Development, and Engineering Center, U.S. Army Missile Command, Redstone Arsenal, Alabama 35898-5248

G. S. Agarwal
School of Physics, University of Hyderabad, Hyderabad-500 134, India

Wolfgang P. Schleich*
Abteilung für Quantenphysik, Universität Ulm, Oberer Eselsberg D-89069 Ulm, Germany
(Received 10 November 1993)

The general theory of quantum angular momentum is used to derive the unique Wigner distribution function for arbitrary angular-momentum states. We give the explicit distribution for atomic angular-momentum Dicke states, coherent states, and squeezed states that correspond to a collection of N two-level atoms. These Wigner functions $W(\theta,\varphi)$ are represented as a pseudoprobability distribution in spherical phase space with spherical coordinates θ and φ on the surface of a sphere of radius $\hbar\sqrt{j(j+1)}$ where j is the total angular-momentum eigenvalue.

PACS number(s): 42.50.Dv, 03.65.Bz, 31.15.+q

I. INTRODUCTION

The harmonic-oscillator phase-space description of electromagnetic fields has had great success in leading to an understanding of the relationship between semiclassical and quantum theories of light. It was Sudarshan [1] who proved the optical equivalence theorem, i.e., he derived the relationship between the quantities measured by a photodetector and the mean values of the corresponding operators. He showed that the function appearing in the diagonal coherent-state representation that is calculated from the density matrix provides a link between the semiclassical and quantum descriptions. This so-called P distribution, now denoted by $P(\alpha)$, is generally singular for nonclassical states [2]. In such cases, the Wigner function [3,4] has proved to be especially attractive as an alternative. The Wigner function in harmonic-oscillator phase space has also proved to be quite useful in discussing related topics such as the photon-number distribution and phase distribution. In these problems, the concept of the area of overlap in phase space has been especially useful [5].

The nonclassical characteristics of atomic systems, such as a collection of two-level atoms, or the treatment of bosonic or fermionic atoms in an atom trap or atom interferometer, has been a subject of much investigation [6,7]. Much of the work has concentrated on the direct calculation of the variances in the N-atom angular-momentum operators such as $\hat{J}_x$ and J_+, and J_-. Very little has been done on the relationship between the nonclassical aspects and the angular-momentum spherical phase-space distributions for such atomic operators. For general angular-momentum systems, Arecchi *et al.* [8] introduced the analog of the diagonal coherent-state representation

$$\hat{\rho}=\int P(\alpha,\beta)|\alpha,\beta\rangle\langle\alpha,\beta|d\Omega\ , \tag{1}$$

where $|\alpha,\beta\rangle$ represents the atomic coherent state

$$|\alpha,\beta\rangle=\sum_{m=-j}^{+j}\left[\begin{matrix}2j\\ j+m\end{matrix}\right]^{1/2}\left[\sin\frac{\alpha}{2}\right]^{j+m}\left[\cos\frac{\alpha}{2}\right]^{j-m}\times e^{-i(j+m)\beta}|jm\rangle\ , \tag{2}$$

and where $|jm\rangle$ is the Dicke eigenstate of $\hat{J}^2$ and $\hat{J}_z$. As usual, the differential of spherical angle is given by $d\Omega\equiv\sin\alpha\, d\alpha\, d\beta$. Arecchi *et al.* discussed the utility of the function $P(\alpha,\beta)$ in atomic problems, and Scully and co-workers have discussed the Wigner function for spin-$\frac{1}{2}$ particles [9]. Using the general theory of multipole operators [10], Agarwal introduced the Wigner function for systems of arbitrary angular momentum in spherical phase space [11]. To arrive at this distribution, we first expand an arbitrary atomic or angular-momentum operator $\hat{G}$ as

$$\hat{G}=\sum_{k=0}^{2j}\sum_{q=-k}^{+k}G_{kq}\hat{T}_{kq}\ , \tag{3}$$

where $\hat{T}_{kq}$ is the multipole operator defined by

$$\hat{T}_{kq}=\sum_{m=-j}^{j}\sum_{m'=-j}^{+j}(-1)^{j-m}\sqrt{2k+1}\left[\begin{matrix}j & k & j\\ -m & q & m'\end{matrix}\right]\times|jm\rangle\langle jm'|\ , \tag{4}$$

where $\left[\begin{matrix}j & k & j\\ -m & q & m'\end{matrix}\right]$ is the usual Wigner $3j$ symbol [10]. The expansion coefficients G_{kq} in the atomic operation expansion Eq. (3) are obtained from the orthogonality of the multipole operators

$$G_{kq}=\mathrm{Tr}\left[\hat{G}\hat{T}^{\dagger}_{kq}\right]\ . \tag{5}$$

*Also at: Max-Planck-Institut für Quantenoptik, D-85748 Garching bei München, Germany.

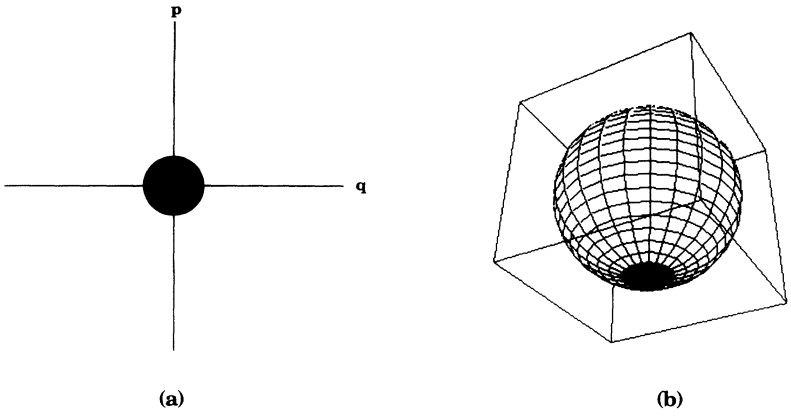

(a) (b)

FIG. 1. The standard schematic depiction of the harmonic-oscillator ground state $|n\rangle=|0\rangle$ as a disk at the origin is shown in (a). This should be compared to the analogous spherical phase-space depiction of the Dicke ground state $|jm\rangle=|j,-j\rangle=|5,-5\rangle$ as a circular cap at the south pole (b). The sphere has a radius $\hbar\sqrt{j(j+1)}=\hbar\sqrt{30}$.

The Wigner function associated with the atomic operator $\hat{G}$ is then defined uniquely by [11]

$$W(\theta,\varphi)=\sum_{k=0}^{2j}\sum_{q=-k}^{+k}Y_{kq}(\theta,\varphi)G_{kq}\ , \tag{6}$$

where Y_{kq} are the usual spherical harmonics. This form for W is derived uniquely by requiring that

$$\mathrm{Tr}\hat{G}=\left[\frac{2j+1}{4\pi}\right]^{1/2}\int W(\theta,\varphi)d\Omega\ , \tag{7}$$

and by requiring further that if two operators $\hat{G}^{(1)}$ and $\hat{G}^{(2)}$ are represented, respectively, by the Wigner functions $W^{(1)}$ and $W^{(2)}$, then

$$\mathrm{Tr}[\hat{G}^{(1)}\hat{G}^{(2)}]=\int W^{(1)}(\theta,\varphi)W^{(2)}(\theta,\varphi)d\Omega\ . \tag{8}$$

Thus, unlike the P function, the expectation values can be obtained in terms of the Wigner functions alone.

In this paper we shall consider the structure of the Wigner function associated with important states such as nonclassical Dicke states $|j,m\rangle$, classical coherent states $|\alpha,\beta\rangle$, given by Eq. (2), and nonclassical squeezed states $|\zeta,m\rangle$. In particular, we will discuss the squeezed atomic state associated with a collection of N two-level atoms immersed in a squeezed photon bath. We examine how the quantum character of the state reflects itself in the properties of the Wigner function by plotting the distribution $f(\theta,\varphi)\equiv 1+W(\theta,\varphi)/[\hbar\sqrt{j(j+1)}]$ in spherical phase space.

II. ANGULAR-MOMENTUM DICKE STATES $|jm\rangle$

Dicke states $|jm\rangle$ are the spherical phase-space analog of the Fock states $|n\rangle$ in harmonic-oscillator phase space. For the Fock states $|n\rangle$, we have $n=0,1,2,\ldots$. The vacuum state $|0\rangle$ is represented by a disk at the origin, and an excited state $|n\rangle$, $n>0$, is represented by an annulus. Similarly, for fixed j, the Dicke ground state $|j,-j\rangle$ is represented by a cap at the south pole in spherical phase space, and an excited state $|j,m\rangle$, $m>-j$, is an annulus [5]. These schematic depictions are illustrated in Figs. 1 and 2.

The location of the annuli in spherical phase space can be determined by the classical angular-momentum vectors associated with the $\hat{J}_z$ eigenvalues m [12], as shown in Fig. 3. Each annulus corresponds to a single vector. At the poles the annuli close in to form caps, just as in harmonic-oscillator space where the ground-state annulus closes in to form the disk representing $|n\rangle=|0\rangle$.

A harmonic-oscillator Fock state $|n\rangle$ has a well-

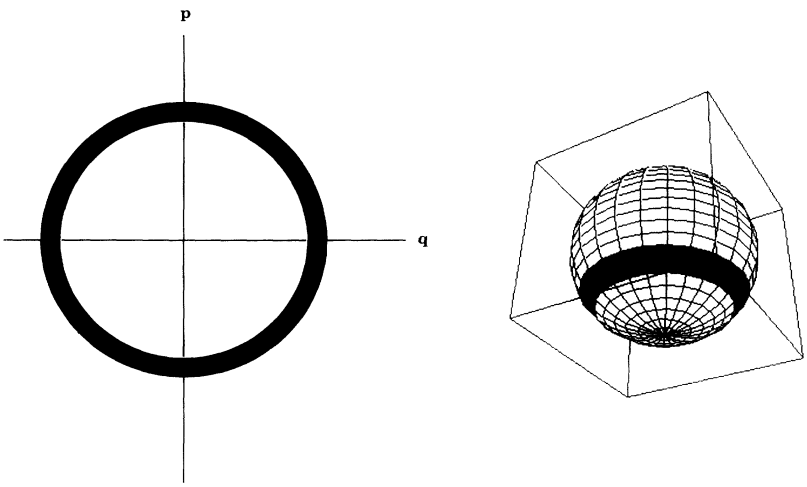

(a) (b)

FIG. 2. An excited oscillator state $|n\rangle=|2\rangle$ is depicted in (a) as an annular region in phase space. Analogously, an excited Dicke state $|j,m\rangle=|5,-2\rangle$ is shown as an annular region in spherical phase space. Both states have a totally imprecise phase φ ranging over $\varphi\in[-\pi,\pi)$.

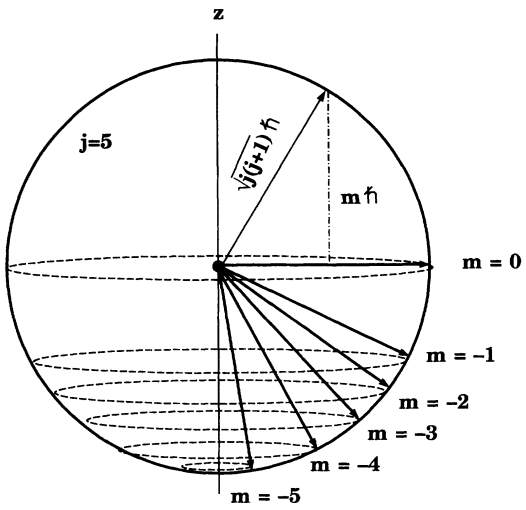

FIG. 3. Here we show a schematic diagram of the classical angular-momentum vector for the Fock states inside a sphere of radius $\hbar\sqrt{j(j+1)}$. The vectors have all length $\hbar\sqrt{j(j+1)}$, but a z component $m\hbar$. These vector locations correspond to the maximal contributions from the Wigner functions shown in Fig. 4. In particular, the Wigner function always has an uncanceled dominant peak at precisely these locations in the angle θ. They fix the location of the bands of a surface area in phase space, depicted in 2(b).

defined excitation number n. Hence, by the oscillator number-phase uncertainty relation $\Delta n\Delta\varphi\gtrsim 1$, the phase is totally indeterminate and $\varphi\in[-\pi,\pi)$. This explains why the phase-space area is an annulus centered at the origin. In a similar fashion, in angular-momentum phase space, a Dicke state $|jm\rangle$ has a well-defined angular momentum in the z direction. Hence, $\langle\hat{J}_x\rangle$ and $\langle\hat{J}_y\rangle$ are completely indeterminate [10]. Since this translates to complete ignorance of the azimuthal angle φ, once again the appropriate representation in phase space is an annulus—this time on a sphere.

The Wigner distribution quantifies our notion of these areas in phase space. We first obtain the Wigner function for the Dicke state $|jm\rangle$. The density-matrix operator $\hat{\rho}$ can be written in the form

$$\hat{\rho}=|jm\rangle\langle jm| \ . \tag{9}$$

Upon using Eqs. (4)–(6) defining the Wigner distribution, we find that

$$W_{jm}^{\text{Dicke}}(\theta,\varphi)=\sum_{k=0}^{2j} Y_{k0}(\theta,\varphi)(-1)^{j-m}\sqrt{2k+1}\times\begin{bmatrix} j & k & j \\ -m & 0 & m\end{bmatrix}^{*} . \tag{10}$$

As expected by symmetry considerations, W_{jm} is independent of φ.

This function is plotted in Fig. 4 as a function of $\theta\in[0,\pi]$ and $\varphi\in[-\pi,\pi)$ for $j=5$ and $m=0,-1,\ldots,-5$. We plot the distribution both as a planar surface and as a spherical surface of the form $f(\theta,\varphi)\equiv 1+W(\theta,\varphi)/[\hbar\sqrt{j(j+1)}]$. If we suppose that $|jm\rangle$ is an orbital-angular-momentum state, then quantum mechanically we would expect the angular-momentum vector of length $\hbar\sqrt{j(j+1)}$ to be oriented inside a sphere of the same radius such that the vector's z component is $m\hbar$. This situation is depicted in Fig. 3, with $j=5$ and $m=0,-1,-2,\ldots,-5$. The Wigner function $W(\theta,\varphi)$, when integrated over the domain of spherical angle, $\theta\in[0,\pi]$ and $\varphi\in[-\pi,\pi)$, contributes the most positive probability at precisely these locations in θ corresponding to the classical vectors. At these θ values there is always one peak on the "wavy sea" that is not canceled by a trough, and so contributes a large amount of probability. This peak is a quantitative association for the area enclosed by the annular bands. In Fig. 4 we plot the function $W(\theta,\varphi)$ as a two-dimensional surface, and also the normalized function $f(\theta,\varphi)\equiv 1+W(\theta,\varphi)/[\hbar\sqrt{j(j+1)}]$ in spherical coordinates, so that the oscillations can be viewed as variations in the surface of a sphere of radius one.

III. ATOMIC COHERENT STATE $|\alpha,\beta\rangle$

In harmonic-oscillator phase space, the ground state $|n\rangle=|0\rangle$ is a coherent state represented by a disk at the origin to indicate variances, $\langle(\Delta x)^2\rangle=\langle(\Delta y)^2\rangle$. Similarly, the spherical phase-space ground state $|jm\rangle=|j,-j\rangle$ is a coherent state represented by a cap on the south pole to represent equal variances, $\langle(\Delta J_x)^2\rangle=\langle(\Delta J_y)^2\rangle=\frac{1}{2}|\langle\hat{J}_z\rangle|$ (see Fig. 1). Now a general harmonic-oscillator coherent state $|\alpha\rangle$, of mean excitation number $|\alpha|^2$, can be obtained by a simple displacement operation, i.e., $|\alpha\rangle=\hat{D}_\alpha|0\rangle$. Here, $\hat{D}_\alpha$ is the usual coherent-state displacement operator [5]. In direct analogy, a general spherical coherent state $|\alpha,\beta\rangle$ is obtained by rotating the ground state off the south pole, $|\alpha,\beta\rangle=\hat{R}_{\alpha\beta}|j,-j\rangle$, where $\hat{R}_{\alpha\beta}$ is the generalized rotation operation [8,10,11], given in terms of the raising and lowering operators $\hat{J}_\pm$ by $\hat{R}_{\alpha\beta}\equiv\exp[\alpha(e^{-i\beta}\hat{J}_+-e^{+i\beta}\hat{J}_-)]$. These rotations are depicted schematically in Fig. 5. Now to quantify these ideas, we again turn to the Wigner distribution.

We consider the Wigner function for the atomic coherent state $|\alpha,\beta\rangle$, Eq. (2), whose density matrix is given by

$$\hat{\rho}=|\alpha,\beta\rangle\langle\alpha,\beta| \ . \tag{11}$$

Using Eq. (2) for the expansion of the coherent state $|\alpha,\beta\rangle$ in terms of Dicke states $|jm\rangle$, and Eqs. (4) and (5) defining the multipole expansions, the coefficients G_{kq} for the density-matrix operator $\hat{\rho}$, Eq. (11), are found to be

$$G_{kq}^{\text{coherent}}=e^{-iq\beta}(\tan\alpha/2)^q\sum_{m=-j}^{j}\left[\frac{2j}{j+m}\right]^{1/2}\left[\frac{2j}{j+m+q}\right]^{1/2}(\sin\alpha/2)^{2j+2m}(\cos\alpha/2)^{2j-2m}(-1)^{j-m-q}(2k+1)^{1/2}\times\begin{bmatrix} j & j & k \\ m & -m-q & q\end{bmatrix} . \tag{12}$$

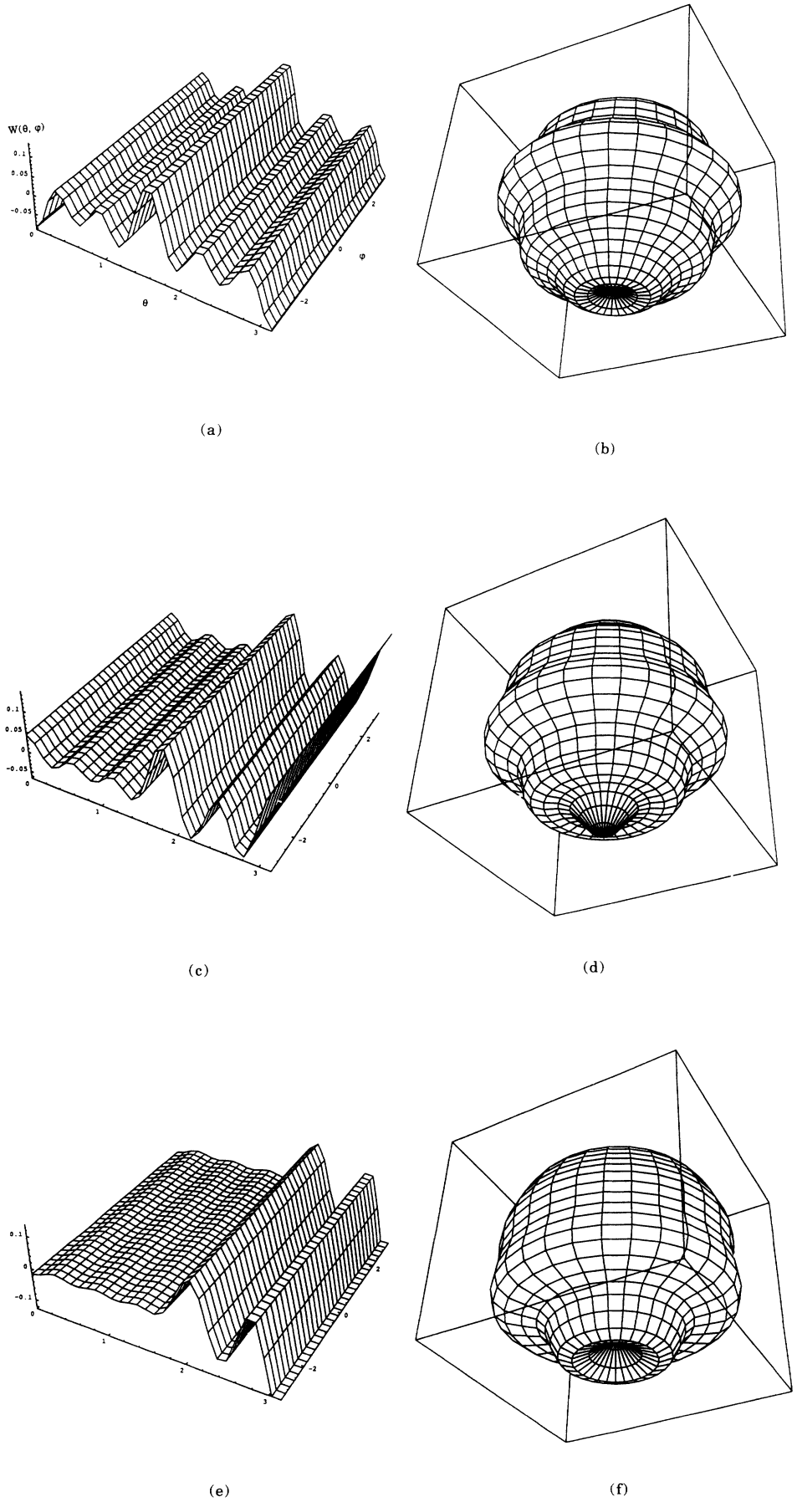

FIG. 4. Here for $\theta\in[0,\pi]$ and $\varphi\in[-\pi,\pi)$ we plot the normalized Wigner function $f(\theta,\varphi)\equiv 1+W^{\text{Dicke}}(\theta,\varphi)/[\hbar\sqrt{j(j+1)}]$, where $W^{\text{Dicke}}(\theta,\varphi)$ is given by Eq. (10). The angular-momentum Dicke states represented here are $|jm\rangle=|5,m\rangle$, where $m=0,-1,-2,-3,-4$, and -5, for (a), (b); (c), (d); (e), (f); (g), (h); (i), (j); and (k), (l); respectively. When integrated over θ, the Wigner function contributes the most positive probability precisely at the locations where the angular-momentum vector for $|jm\rangle$ of length $\hbar\sqrt{j(j+1)}$ has a z component $m\hbar$ (see Fig. 2). These contributions occur where the dominant positive crest of the Wigner function—the peak that is not canceled by any troughs—contributes. At the poles the distribution fills in to form a cap, analogous to harmonic-oscillator space where the ground state fills in and is represented by a disk, and not an annulus (see Fig. 1). To bring out all the features of $W(\theta,\varphi)$, we plot it first as a two-dimensional surface function of $W(\theta,\varphi)$ in (a), (c), (e), (g), (i), and (k). This method of presentation brings out the scale of the local positive and negative variations of W with respect to the plane $f(\theta,\varphi)\equiv 0$. Then in (b), (d), (f), (h), (j), and (l), we take a global view by plotting $f(\theta,\varphi)\equiv 1+W(\theta,\varphi)/[\hbar\sqrt{j(j+1)}]$ on a sphere of radius one.

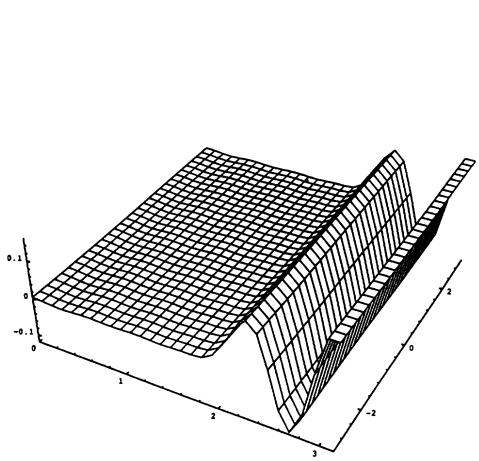

(g)

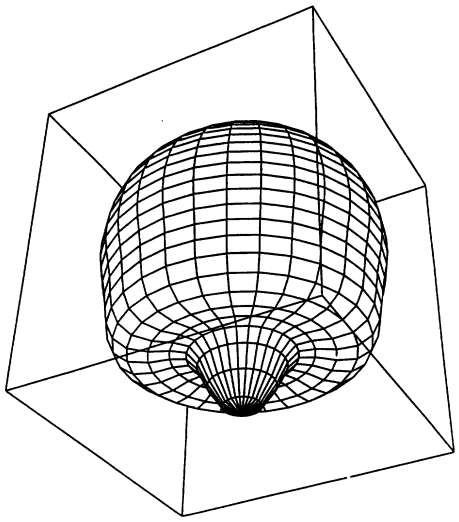

(h)

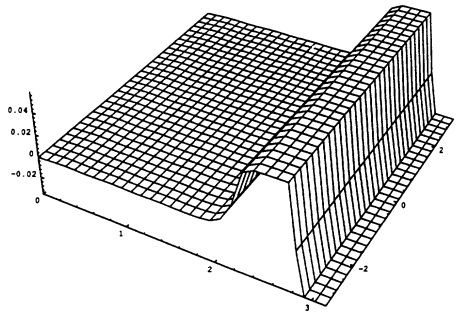

(i)

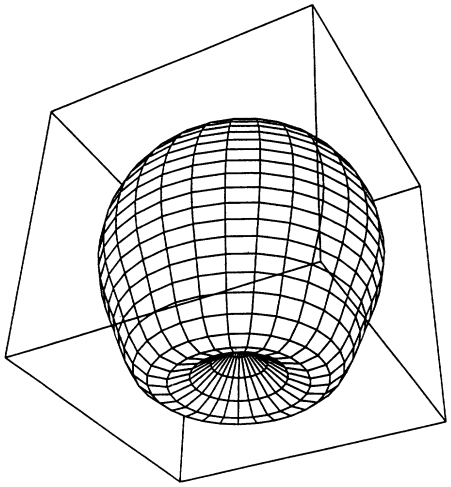

(j)

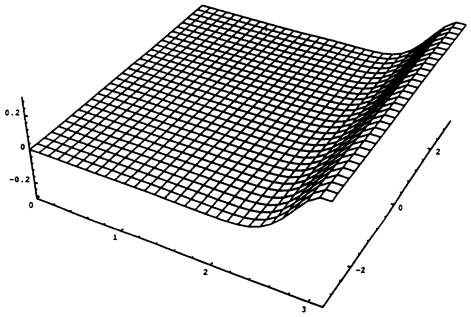

(k)

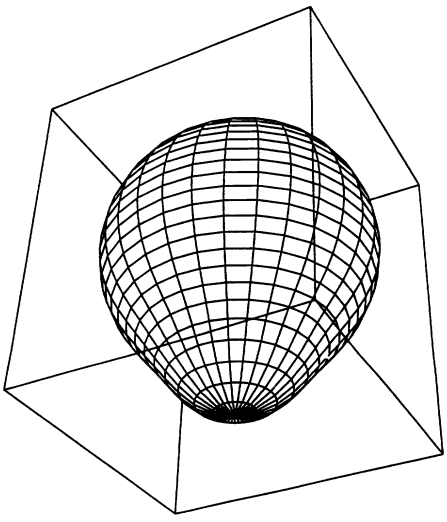

(l)

FIG. 4. (*Continued*).

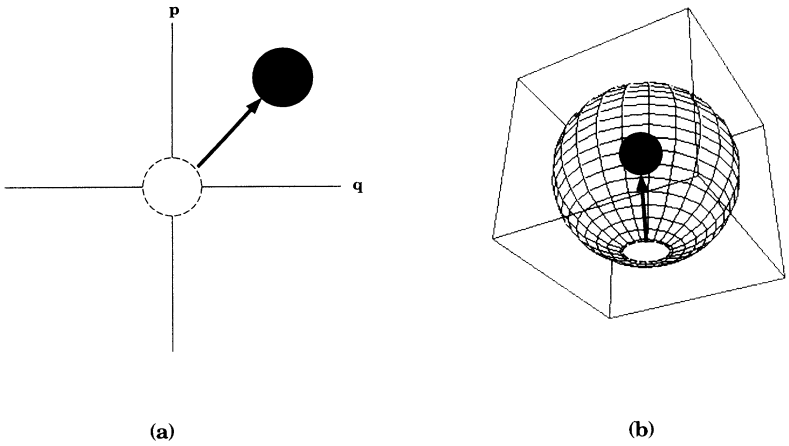

FIG. 5. The harmonic-oscillator ground state $|n\rangle=|0\rangle$ is a special case of a coherent state. As shown in (a), a general harmonic-oscillator coherent state $|\alpha\rangle$ can be generated by displacing the ground state $|\alpha\rangle=\hat{D}_\alpha|0\rangle$, where $\hat{D}$ is the usual coherent-state displacement operator. Similarly, a general spherical coherent state $|\alpha,\beta\rangle$ can be obtained by rotating the coherent Dicke ground state $|jm\rangle=|j,-j\rangle$ off the south pole. We show such a state, $|\alpha,\beta\rangle=\hat{R}_{\alpha\beta}|j,-j\rangle$, in (b), where $\hat{R}$ is the spherical angular rotation operator.

The Wigner function $W^{\rm coh}(\theta,\varphi)$ is then given by Eq. (6), and is plotted in Fig. 6 for a rotation to $\alpha=\beta=\pi/4$, where α is measured off the south pole [8]. (Again we plot $f(\theta,\varphi)\equiv 1+W(\theta,\varphi)/[\hbar\sqrt{j(j+1)}]$.) The coherent state appears as a positive perturbation on the surface of a unit sphere. It is a Gaussian distribution located on the sphere's surface at $\theta=3\pi/4,\varphi=\pi/4$. The Gaussian shape is analogous to that found for the Wigner distribution for coherent states of the single-mode radiation field corresponding to a harmonic-oscillator coherent state [5]. The coherent state is a minimum uncertainty state in the sense that it yields an equality for the Heisenberg angular-momentum uncertainty relation

$$\langle(\Delta J_{x'})^2\rangle\langle(\Delta J_{y'})^2\rangle\geq\tfrac{1}{4}|\langle\hat{J}_{z'}\rangle|^2\ ,$$

where $\hat{J}_{x'}$, $\hat{J}_{y'}$, and $\hat{J}_{z'}$ are computed in a rotated coordinate system, where z' is an axis in the (α,β) direction through the center of the coherent state [8,10]. The variances $\Delta J_{x'}$ and $\Delta J_{y'}$ measure fluctuation about this axis. For a coherent state, the minimum-uncertainty condition is $\langle(\Delta J_{x'})^2\rangle=\langle(\Delta J_{y'})^2\rangle=\frac{1}{2}|\langle\hat{J}_{z'}\rangle|$, and the fluctuations are symmetric about the z' axis. This is why we represent the state by a circular cap centered at (α,β).

As we mentioned above, the Wigner distribution of a coherent state at the south pole is identical to that of the ground or vacuum Dicke state $|j,m\rangle=|j,-j\rangle$. The distribution of any other coherent state may be obtained by rotation on the phase-space sphere—analogous to displacement in the harmonic-oscillator phase-space plane, Fig. 5. A cross section through $W(\theta,\varphi)$ tangent to the

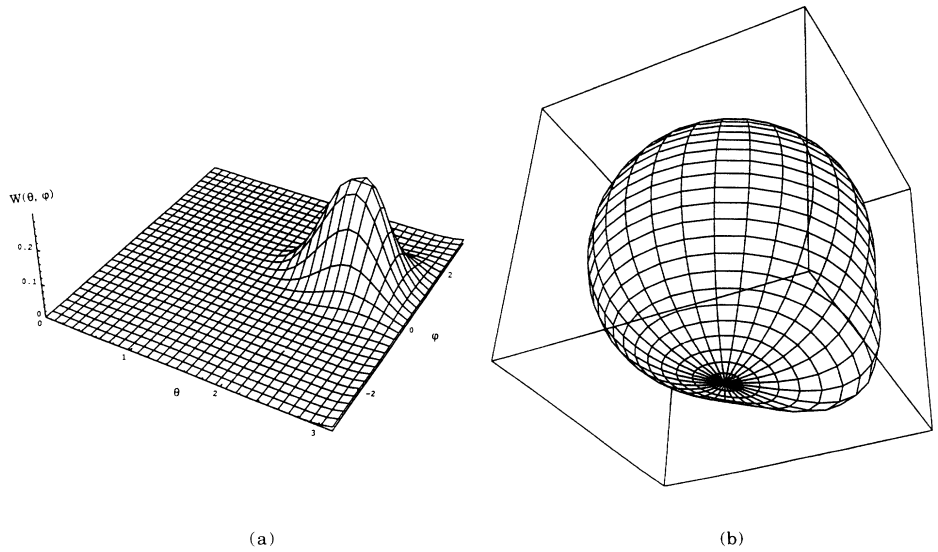

FIG. 6. Here we plot the Wigner distribution $W^{\rm coh}/\hbar\sqrt{j(j+1)}$ for the coherent state $|\alpha,\beta\rangle$, Eq. (2). We choose parameters $\alpha=\beta=\pi/4$ that correspond to a Gaussian distribution localized at $\theta=-\pi/4,\varphi=\pi/4$. (The angle α is measured off the south pole.) This distribution is qualitatively similar to that of the harmonic-oscillator coherent state. Again we present a two-dimensional surface view (a) and a spherical coordinate perspective (b). This state obeys the minimal uncertainty relation and $\langle(\Delta J_{x'})^2\rangle=\langle(\Delta J_{y'})^2\rangle=\frac{1}{2}\langle(\hat{J}_{z'})^2\rangle^{1/2}$, where the prime coordinates are rotated such that z' passes through the center of the coherent state. This distribution should be compared to the schematic disk representation in Fig. 5(b).

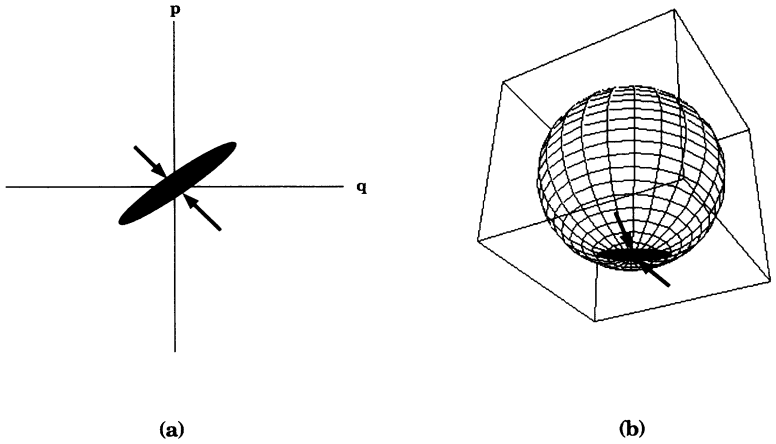

(a) (b)

FIG. 7. A squeezed harmonic-oscillator vacuum state $|\zeta\rangle=\hat{S}_\zeta|0\rangle$ is shown in (a), where $\hat{S}$ is a typical squeezing operator. The analogous squeezed angular momentum ground state $|\zeta\rangle=\hat{S}_\zeta=|j,-j\rangle$ is depicted in (b).

sphere at (α,β) will always be circular for a coherent state.

IV. ATOMIC SQUEEZED STATE

We compare the squeezed harmonic-oscillator vacuum state $|0,\zeta\rangle=\hat{S}_\zeta|0\rangle$ to the squeezed angular-momentum ground state $|\zeta\rangle=\hat{S}_\zeta=|j,-j\rangle$ in Fig. 7. The squeezed state is represented schematically by an ellipse in oscillator space and by an elliptical cap in spherical space. For the oscillator, a displacement may be applied after squeezing to generate a general squeezed state $|\alpha,\zeta\rangle=\hat{D}_\alpha\hat{S}_\zeta|0\rangle$. For the sphere, a rotation $\hat{R}$ is applied after squeezing to generate a more general squeezed coherent state $|\alpha,\beta,\zeta\rangle=\hat{R}_{\alpha\beta}\hat{S}_\zeta|j,-j\rangle$. These states are depicted in Fig. 8. In addition, there are squeezed Dicke states given by applying $\hat{S}$ to $|jm\rangle$, where m is not necessarily equal to $-j$. However, if $m=-j$, then the squeezed Dicke state reduces to the squeezed coherent ground state [11]. We now quantify this phase-space representation, again with the definition of our spherical Wigner function.

We then consider the Wigner distribution state [13,14] of the angular-momentum state defined by

$$|\zeta,m\rangle=\mathcal{A}_m\exp(\Theta\hat{J}_z)\exp(-i\pi\hat{J}_y/2)|jm\rangle\ , \tag{13}$$

where $\mathcal{A}_m$ is the normalization constant. This state—a squeezed Dicke state—represents a collection of two-level atoms exposed to a squeezed radiation bath. In this state the x quadrature, i.e., $\hat{J}_x$, is squeezed, since

$$\langle(\Delta J_x)^2\rangle=\tfrac{1}{2}|\langle\hat{J}_z\rangle|e^{-|\zeta|}<\tfrac{1}{2}|\langle\hat{J}_z\rangle|\ , \tag{14}$$

where the squeezing parameter ζ is defined implicitly by

$$e^{2\Theta}=\tanh(2|\zeta|)\ . \tag{15}$$

Thus the squeezed Dicke states of Eq. (13) can be considered suitable candidates for squeezed states of the general angular-momentum system. In addition, Agarwal and Puri [13] have shown that the states of Eq. (13) are the eigenstates of the operator $(J_-\cosh|\zeta|+J_+\sin|\zeta|)/\sqrt{2\sinh 2|\zeta|}$, with the eigenvalue m, and that these states are the analog of the two-photon coherent states [2] for photons. Note further that Eq. (13) for the squeezed Dicke state can be written in terms of the elements of the rotation operator $d^j_{mm'}(\pi/2)$, defined implicitly by

$$\langle jm|\zeta p\rangle=\mathcal{A}_p e^{m\Theta}d^j_{mp}(\pi/2)\ , \tag{16}$$

where, explicitly, we have

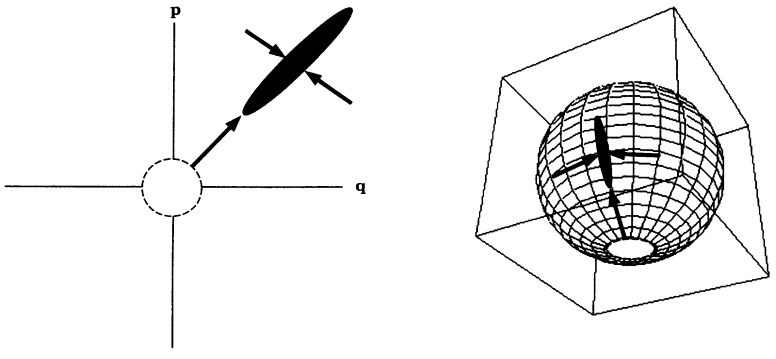

(a) (b)

FIG. 8. A general squeezed coherent state, shown in (a), is the product of a squeezing $\hat{S}$ and a displacement $\hat{D}$ of the ground state in harmonic-oscillator phase space, $|\alpha,\zeta\rangle=\hat{S}_\zeta\hat{D}_\alpha|0\rangle$. In (b) we depict a general squeezed coherent angular-momentum state $|\alpha,\beta,\zeta\rangle=\hat{S}_\zeta\hat{R}_{\alpha\beta}|j,-j\rangle$ that is the product of a squeezing $\hat{S}$ and a rotation $\hat{R}$ in spherical phase space.

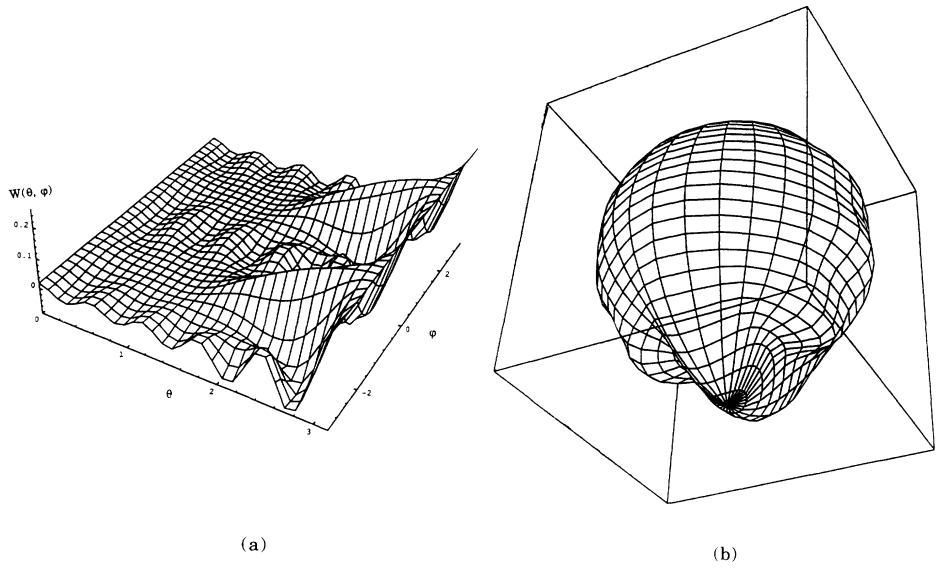

FIG. 9. Here we plot the Wigner function for a squeezed angular-momentum Dicke ground state $|\zeta,-5\rangle$ defined by Eq. (13). The function $W^{\rm squ}(\theta,\varphi)$ is computed using Eqs. (6), (17), and (18) for a squeezing parameter of $\theta=-2.13\times10^{-5}$ corresponding to a mean occupation number of $\bar{n}=50$. In (a) we plot the function as a surface $W(\theta,\varphi)$ as before. We have normalized the variation in the surface in spherical coordinates to a sphere of radius $\hbar\sqrt{j(j+1)}$ in (b), so that the elongated Gaussian appears here as a "Wigner banana" draped across the surface of the sphere of radius one at the south pole. Notice that the squeezed state is more localized in the x direction at the expense of decreased localization or increased noise in the y direction. This corresponds to a decreased uncertainty in $\langle(\Delta J_x)^2\rangle$ as given in Eq. (14).

$$d^j_{mp}(\pi/2)=\frac{((j+m)!(j-m)!(j+p)!(j-p)!)^{1/2}}{2^j}\sum_{q=-j}^{+j}\frac{(-1)^q}{(j-p-q)!q!(q+p-m)!(j+m-q)!}\ . \tag{17}$$

Upon using Eqs. (13), (16), and (17) in the Wigner equations (4) and (5), we find the squeezed state expansion coefficients G_{kq} to be

$$G^{\rm squeezed}_{kq}=\sum_{m=-j}^{j}\sum_{m'=-j}^{j}(-1)^{j-m}(2k+1)^{1/2}\begin{pmatrix} j & k & j\\ -m & q & m'\end{pmatrix}\left[\frac{e^{(m+m')\Theta}d^j_{mp}d^j_{m'p}}{\sum_{m''}|d^j_{m''p}|^2e^{2m''\Theta}}\right], \tag{18}$$

where we have also introduced the value of the normalization constant. The Wigner distribution $W^{\rm squ}(\theta,\varphi)$ obtained from Eq. (6), using Eqs. (17) and (18), is plotted in Fig. 9 for $j=5$ and $p=-5$. This corresponds to squeezing the Dicke ground-state coherent state $|\alpha,\beta\rangle=|jm\rangle=|5,-5\rangle$ at the south pole of phase space. We take the squeezing parameter Θ equal to -2.13×10^{-5} which corresponds to a mean occupation number of $\bar{n}=\sinh^2(\frac{1}{2}\text{arctanh}(e^{2\Theta}))=50$. The plot is again normalized so that the elongated Gaussian of the squeezed state appears as a "Wigner banana" draped across the surface of sphere of radius one at the south pole. [To see this, one must take the surface in Fig. 9(a) and mentally map it onto a sphere of radius one, as in Fig. 9(b).] Notice that the localization of the state is squeezed in the x direction at the expense of knowledge about the y location, in accordance with Eq. (14). Agarwal and Puri [13] have shown how the squeezed Dicke atomic states given by Eq. (13) can be produced if a collection of two-level atoms interacts with a broad band squeezed vacuum photon bath, and if one concentrates only on the steady-state solution for the collective system. The parameter ζ characterizes the squeezed bath with average photon number equal to $\sinh^2\zeta$.

V. CONCLUSION

In summary, the Wigner distribution for a general angular-momentum state has been derived and explicitly given for a Dicke state, a general coherent state, and a squeezed ground state. Represented as a pseudoprobability distribution on the sphere of radius one in angular-momentum phase space, the Wigner function is plotted for these three situations. These plots enable us to understand the nonclassical nature of the states of a collection of identical two-level atoms, since the collection is described by the addition of the spin operators for each atom. In addition, this formalism applies equally well to any collection of fermions or bosons in, say, an atomic trap or atom interferometer [7].

ACKNOWLEDGMENTS

Both G.S.A. and J.P.D. thank Professor H. Walther for his hospitality and support at the Max-Planck-Institut für Quantenoptik, where part of this work was done. G.S.A. also acknowledges travel support under the National Science Foundation Grant No. INT 9100685, and one of us (J.P.D.) would like to acknowledge the National Research Council of the United States for support. We would like to thank M. Benedict, D. Heinzen, S. Stenholm, and D. J. Wineland for many fruitful discussions, and H. Wolter for the use of a program for evaluating the Wigner 3-*j* symbols.

[1] E. C. G. Sudarshan, Phys. Rev. Lett. **10**, 277 (1963); see also R. J. Glauber Phys. Rev. **131**, 2766 (1963).

[2] H. P. Yuen, Phys. Rev. A **13**, 2226 (1976); for many important properties of *P* function, see R. J. Glauber in Ref. 1.

[3] E. P. Wigner, Phys. Rev. **40**, 749 (1932).

[4] G. S. Agarwal, J. Mod. Opt. **34**, 909 (1987); M. Hillery, R. F. O'Connell, M. O. Scully, and E. P. Wigner, Phys. Rep. **106**, 121 (1984).

[5] For a comprehensive account of the area of overlap method in harmonic-oscillator phase space, see J. P. Dowling, W. P. Schleich, and J. A. Wheeler, Ann. Phys. (Leipzig) **48**, 423 (1991); for use of area of overlap in spherical angular-momentum phase space, see M. Benedict (private communication); C. C. Lassig and G. J. Milburn, Phys. Rev. A **48**, 1854 (1993).

[6] K. Wódkiewicz and J. H. Eberly, J. Opt. Soc. Am. B **2**, 458 (1985); see also P. K. Arvind, *ibid.* **5**, 1545 (1988).

[7] N. Rehler and J. H. Eberly, Phys. Rev. A **2**, 1607 (1970); M. Kitagawa and M. Veda, Phys. Rev. Lett. **67**, 1852 (1991); D. J. Wineland *et al.*, Phys. Rev. A **46**, R6797 (1992); B. Yurke, Phys. Rev. Lett. **56**, 1515 (1986); M. O. Scully and J. P. Dowling, Phys. Rev. A **48**, 3186 (1993).

[8] F. T. Arecchi, E. Courtens, R. Gilmore, and H. Thomas, Phys. Rev. A **6**, 2211 (1972). For a detailed review on the coherent states for various systems, see A. M. Perelomov, Usp. Fiz. Nauk. **123**, 23 (1977); [Sov. Phys. Usp. **20**, 703 (1977)].

[9] L. Cohen and M. O. Scully, Found. Phys. **16**, 295 (1986); M. O. Scully, Phys. Rev. D **28**, 2477 (1983); L. Cohen and M. O. Scully, in *New Techniques and Ideas in Quantum Measurement Theory,* edited by D. Greenberger, special issue of Ann. N.Y. Acad. Sci. **480**, 115 (1987); M. O. Scully and K. Wódkiewicz, in *Coherence and Quantum Optics VI,* edited by J. H. Eberly *et al.* (Plenum, New York, 1990), p. 1047.

[10] A. R. Edmonds, *Angular Momentum in Quantum Mechanics* (Princeton University Press, Princeton, NJ, 1957), Sec. 3.7.

[11] G. S. Agarwal, Phys. Rev. A **24**, 2889 (1981).

[12] F. K. Richtmyer, E. H. Kennard, and J. N. Cooper, *Introduction to Modern Physics,* 6th ed. (McGraw-Hill, New York, 1969), Sec. 14.5.

[13] G. S. Agarwal and R. R. Puri, Phys. Rev. A **41**, 3782 (1990); Opt. Commun. **69**, 267 (1989).

[14] M. A. Rasheed, J. Math. Phys. **19**, 1391 (1978).